

# Counterbalanced Effect of Surface Trap and Auger Recombination on the Transverse Terahertz Carrier Dynamics in Silicon Nanowires

Chihun In, Jungmok Seo, Hyukho Kwon, Jeongmook Choi, Sangwan Sim, Jaeseok Kim, Taeyong Kim, Taeyoon Lee, and Hyunyong Choi

**Abstract**—The surface-trap mediated carrier recombination is a crucial feature in characterizing the optoelectronic properties of nanowires (NWs). Due to the one-dimensional characteristics, the photoexcited carriers experiences multiple carrier interactions in the transverse direction such that strong carrier-carrier interactions are expected to play an important role in the NW carrier recombination. Here, using ultrafast optical-pump and terahertz-probe spectroscopy, we show that the Auger scattering significantly reduces the trap-mediated decay process. Systematic studies on bulk Si, bundled, individual, and encapsulated (reduced surface-trap density) SiNWs reveal that the effect of Auger recombination exhibits strong pump-fluence dependence depending on the surface-treatment condition.

**Index Terms**—Silicon nanowires, terahertz (THz), ultrafast spectroscopy.

## I. INTRODUCTION

SILICON NANOWIRES (SiNWs) have emerged as attractive nanoscale materials for developing Si-based optoelectronic devices [1]–[4]. Photoexcited carrier dynamics [5]–[7], which limits the performance of Si-based photonic devices [8], [9], is of central importance for NW characterization. In particular, when the SiNWs are transferred onto a target substrate for

device applications, there arises several issues: dependence of the carrier lifetime on the directionality (longitudinal or transverse direction to the NW long axis) [10], the NW–NW interconnection (bundled NW) effect [11], and the inherent surface traps due to the large surface-to-volume ratio [12]. Although various electrical and optical investigations were performed to resolve those effects [13]–[17], the reported carrier lifetime so far is widely ascribed to the longitudinal NW direction, and the lifetime along the transverse direction is barely understood. Furthermore, efforts to reduce the carrier-trap centers via surface encapsulation [18] lead to the enhanced carrier–carrier interaction (multi-particle Auger scattering) under high optical pump injection. Thus, investigation of the carrier lifetime along the transverse direction is equally important because it may reveal a new relaxation pathway of the photoexcited carriers, offering an alternative route toward ultrafast optoelectronic operation.

Prior ultrafast optical studies on the transverse carrier dynamics [11] have focused on the eV-scale, high-energy optical transition dynamics. We note that this optical-pump optical-probe spectroscopy inherently accompanies the photo-induced absorption from the trapped carriers [3], [13], [15]. In order to rule out this effect, we have employed time-resolved low-energy terahertz (THz) spectroscopy. One advantage of the THz spectroscopy is that the carrier excitation from trap levels can be excluded because the surface-trap states are typically located far above the THz-probe photon energy (1 THz = 4.2 meV). Combined with ultrashort optical excitation, the optical-pump and THz-probe spectroscopy enables to investigate the low-energy intrinsic electronic relaxation. In this letter, we aim at investigating the characteristic role of trap-mediated recombination depending on the surface condition and the associated Auger kinetics in carrier dynamics along the transverse NW direction.

For systematic investigation, we performed a series of experiments on three different sets of SiNW samples: bundled SiNWs, individual bare SiNWs, and surface-encapsulated SiNWs. Our measurements reveal that the recombination rate decreases with increasing pump fluence  $F$  for the bundled NWs, while the corresponding rate for the individual bare SiNWs displays an  $F$ -independent feature. This suggests that the effect of surface-trap on the carrier-relaxation decay is different between the two NWs. When the trap-density is reduced (encapsulated NWs), we clearly observe a fast Auger-recombination dynamics whose threshold  $F$ , i.e., the crossover  $F$  from the slow to the fast relaxation, is significantly lower than the case of the bare NWs.

Manuscript received November 06, 2014; revised March 29, 2015; accepted April 22, 2015. Date of publication May 18, 2015; date of current version July 16, 2015. The work of C. In, J. Choi, S. Sim, J. Kim, T. Kim, and H. Choi was supported by National Research Foundation of Korea (NRF) through the government of Korea (MSIP) under Grant NRF-2011-0013255, Grant NRF-2009-0083512, and Grant WCI 2011-001, by the Yonsei University Yonsei-SNU Collaborative Research Fund of 2014, and by the Yonsei University Future-leading Research Initiative of 2014. The work of J. Seo, H. Kwon, and T. Lee was supported by Mid-career Researcher Program through NRF grant funded by the MEST 2014R1A2A2A09053061.

C. In is with School of Electrical and Electronic Engineering, Yonsei University, Seoul 120-749, Korea, and also with Korea Atomic Energy Research Institute, Daejeon 305-353, Korea.

J. Seo, S. Sim, J. Kim, T. Lee, and H. Choi are with School of Electrical and Electronic Engineering, Yonsei University, Seoul 120-749, Korea (e-mail: hychoi@yonse.ac.kr).

H. Kwon was with the School of Electrical and Electronic Engineering, Yonsei University, Seoul 120-749, Korea. He is now with Samsung Electronics Company, Banwolldong, Hwaseongsi, Gyeonggi-do, Korea

J. Choi was with the School of Electrical and Electronic Engineering, Yonsei University, Seoul 120-749, Korea. He is now with LG Display Company, 256, LG-ro, Wollongmyeon, Pajusi, Gyeonggi-do, Korea

T. Kim was with the School of Electrical and Electronic Engineering, Yonsei University, Seoul 120-749, Korea. He is now with the Department of Electrical Engineering, California Institute of Technology, Pasadena, CA 91125 USA

Digital Object Identifier 10.1109/TTHZ.2015.2428619

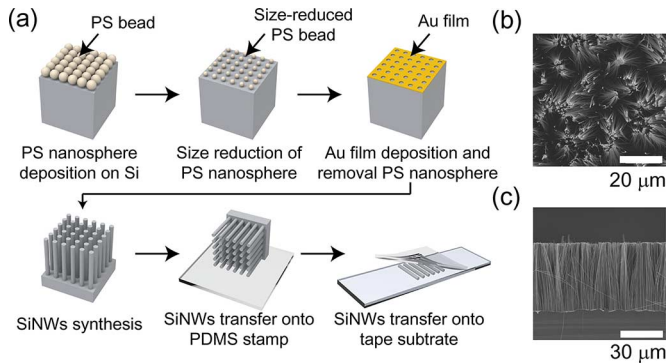


Fig. 1. (a) Schematic of SiNW fabrication employing metal-assisted chemical etching (MACE) combined with Nanosphere Lithography. (b) SEM top-view image of SiNWs. (c) Cross-sectional image of SiNWs.

Analysis based on a simple, two-level rate equation shows that there is a strong correlation between the trap density and the photoexcited carriers.

## II. SiNW SYNTHESIS

SiNWs are synthesized using a metal-assisted chemical etching (MACE) method combined with nanosphere lithography. The detailed information is described elsewhere [19], [20]. In brief, the surface of p-type (100) oriented Si substrate is pre-cleaned with acetone, isopropanol, and de-ionized water, and then immediately dipped into 10% sodium dodecyl sulfate (SDS) solution for 24 hours. On the Si substrate, 10 wt% of polystyrene (PS) nanosphere solution (diameter of 1 μm) is dropped, which is subsequently immersed into water with an addition of the 3 μL SDS solution. Here, a close-packed monolayer of PS nanospheres is formed on the top of the water surface, which is immediately lifted up by the Si substrate. After completely dried under ambient condition, the size of PS nanosphere on Si substrate is reduced by oxygen plasma etching (100 W, 2 sccm, 1 hour), followed by the deposition of 50-nm-thick Au layer. The Si substrate with Au film is immersed into an etching solution consisting of 49% HF, 30% H<sub>2</sub>O<sub>2</sub> and ethanol (5:1:1 (v/v/v) HF: H<sub>2</sub>O<sub>2</sub>: ethanol) for 2 hours at room temperature. After completing the whole process, remaining Au film is removed by aqua regia. The surface encapsulation is synthesized by thermal oxidation of SiNW surface in a furnace at 1000 °C for 4 min to form 5-nm-thick SiO<sub>2</sub> layer [21], [22]. Fig. 1(a) schematically illustrates the fabrication process of vertically aligned SiNWs, using metal-assisted chemical etching method combined with the bottom-up nanosphere lithography. Fig. 1(b) and (c) show the typical top and side view of the synthesized SiNWs, respectively. The as-grown SiNWs are first transferred to the PDMS stamp. At this stage, because there are multiple layers of SiNWs (SiNWs are stacked on top of each other), we used another rigid PDMS stamp to detach the layers of SiNWs until we obtain only one layer of SiNWs sheet. Finally, the obtained one layer of SiNWs is transferred onto a tape substrate, in which we did not observe any significant changes in its vertical alignment for all bundled, individual, and encapsulated SiNWs. Image analysis using optical microscopy revealed that the areal density for bundled, individual, and encapsulated SiNWs is 30%, 3%, and 3%,

respectively. The transferred SiNWs are aligned to the substrate over a broad area with uniform axial lengths (~60 μm) and diameter (~500 nm). The well-aligned SiNWs and good transparent characteristics of the tape substrate (cellophane) in THz region enable to measure the transverse carrier dynamics of SiNWs.

## III. TRANSIENT TERAHERTZ DYNAMICS

Fig. 2(a) shows the schematic of our experiment. All measurements are performed at room temperature in an ambient condition. Our ultrafast THz spectroscopy is based on Ti:sapphire regenerative amplifier (Coherent RegA 9050) operating at 250 kHz repetition rate that generates 50 fs pulses at 1.55 eV center photon energy. Part of the pulses is used to excite the sample, in which the pump polarization is 45 deg to the NW axis due to the following reason. When the wavelength of pump excitation (800 nm) is comparable to the NW diameter, the pump excited carrier density becomes polarization dependent. This can be understood as following. The absorption cross-section of the NW can be calculated by considering the angle between the polarization of optical-pump beam and the longitudinal axis of the NW [11], [23]. Due to the dielectric mismatch between NWs and the surrounding medium, the electric field inside the NW along the transverse direction is given by  $E_{\perp} = (2\epsilon_M/(\epsilon(\omega) + \epsilon_M))E_{0\perp}$ , where  $\epsilon_M$  is the dielectric constant of the surrounding medium,  $\epsilon(\omega)$  is the dielectric constant of the NW, and  $E_{0\perp}$  is the incident electric field polarized along the transverse direction of the NW. When the electric field is polarized parallel to the long axis of NW, the electric field inside the NW is simply given by  $E_{\parallel} = E_{0\parallel}$ , where  $E_{0\parallel}$  is the longitudinal component of the electric field. Given that  $\epsilon_M = 1$  and  $\epsilon(\omega)$  at 1.55 eV is about 13.6 in our experiment [24],  $E_{\perp}$  is about 14% of  $E_{0\perp}$ . Thus, the polarization of pump beam will change the initial density of photoexcited carriers. To circumvent the above polarization dependence, we set the pump polarization to 45° with respect to the longitudinal axis of the NW. In this case, one can consider the angle-averaged absorption cross-section of the NW [25], [26]

$$\sigma_{\text{abs}}(\text{cm}^2) = (\omega/n_1 c)(\pi r^2 l) |f(\omega)|^2 (2n_s k_s) \quad (1)$$

where  $\omega$  is the angular frequency of the pump,  $n_1$  is the refractive index of surrounding medium,  $f(\omega)$  is the local field factor,  $r$  (= 250 nm) and  $l$  (= 60 μm) are the radius and length of the SiNW, and  $n_s$  ( $\cong 3.69$ ) and  $k_s$  ( $\cong 0.0065$ ) are the real and imaginary parts of the bulk Si refractive index at the 800 nm wavelength. The local field factor is related to the electric field inside NW and it is given by

$$f(\omega) = \cos\theta + \frac{2\epsilon_M}{\epsilon_M + \epsilon(\omega)} \sin\theta \quad (2)$$

where  $\theta = 45^\circ$  is the angle between pump polarization and the long axis of NW. From the (1) and (2), the  $\sigma_{\text{abs}}$  at 1.55 eV is estimated to be  $\sigma_{\text{abs}} = 1.43 \times 10^{-8} \text{ cm}^2$ . The absorption cross-section is used later to calculate the photoexcited carrier density.

The excitation  $F$  is controlled by a combination of half-wave plate and polarizer, delivering maximum  $F$  up to 700 μJ/cm<sup>2</sup>. Another part of the amplifier output is used to generate and

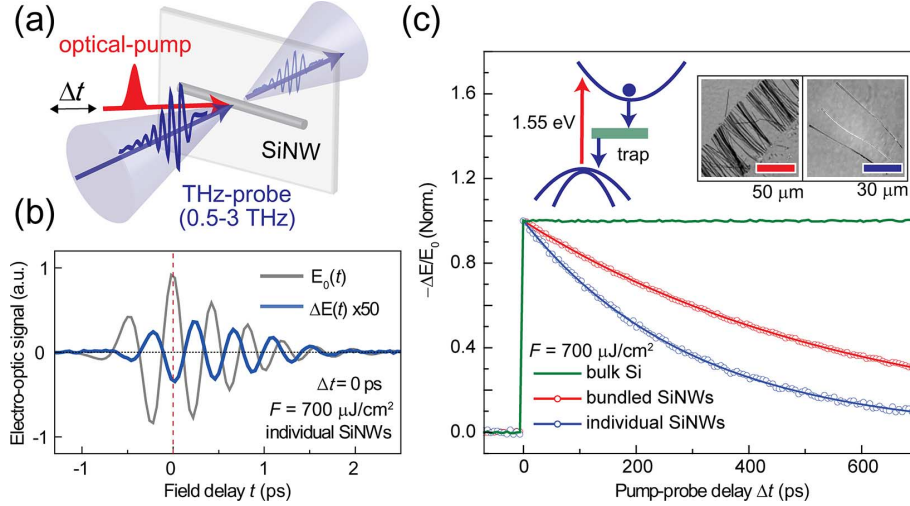


Fig. 2. (a) Schematic of optical-pump terahertz-probe spectroscopy. (b) Reference THz field  $E_0(t)$  (gray line) and pump-induced THz-field change  $\Delta E(t)$  at  $\Delta t = 0$  ps. (c)  $-\Delta E/E_0$  transients as a function of  $\Delta t$ . Insets: Left figure depicts the Si bandstructure for photoinduced carrier excitation and trap-mediated decay. Right figures show the optical microscope images of the bundled SiNWs (red line) and the individual bare SiNWs (blue line).

detect the 0.5–3 THz probe pulses by optical rectification and electro-optic sampling in 0.5 mm thick,  $\langle 110 \rangle$  ZnTe crystals, respectively. To control the THz probe polarization, the NW axis is rotated with respect to the  $s$ -polarized THz pulses. Typical field-resolved THz traces with  $F = 700 \mu\text{J}/\text{cm}^2$  at a pump-probe delay  $\Delta t = 0$  ps is shown in Fig. 2(b). For the pump-probe THz dynamics, we set the THz-field delay  $t$  (electro-optic sampling delay) at the peak of the  $\Delta E(t)$  and scan the pump-probe delay  $\Delta t$ . Non-zero signal changes with opposite signs between the pump-induced THz field  $\Delta E(t)$  and the reference THz field  $E_0(t)$  indicate the transient absorption dynamics of the photoexcited carriers.

To compare the carrier dynamics between the bulk-like and NWs, we first discuss measurements on a set of experiments on bulk Si thin film (500-nm thick) and SiNWs. Fig. 2(c) shows  $-\Delta E/E_0$  dynamics as a function of  $\Delta t$  for bulk Si, bundled SiNWs, and individual bare SiNWs with  $F = 700 \mu\text{J}/\text{cm}^2$ . As depicted in the inset of Fig. 2(c), the interband photoexcited carriers are relaxed by phonon coupling due to the indirect bandstructure of Si. Because the measured photoinduced  $-\Delta E/E_0$  is directly proportional to the carrier density, the decay dynamics at field delay  $t = 0$  ps represents the recombination kinetics of the excited carriers. While the carrier lifetime in bulk Si thin film is on the order of microsecond ( $\mu\text{s}$ ), the decay dynamics for the bundled and the individual SiNWs are significantly faster than that of the bulk Si. This is because the excited carriers in SiNWs (both bundled and individual) are rapidly recombined via defect trapping [11], [12], [15], [27], [28]. Although this rapid carrier relaxation occurs due to the high density of trap states, the signal for individual SiNWs decreases more quickly than that of the bundled NWs.

#### IV. SURFACE TRAP SATURATION AND AUGER RECOMBINATION

To gain more insight into the role of defects on the decay dynamics, we present the  $F$ -dependent  $-\Delta E/E_0$  data for the bundled SiNWs in Fig. 3(a) and those for the individual SiNWs in

Fig. 3(b), respectively. We noticed that both a single exponential fit and the rate-equation fit (to be discussed in Section V) well reproduce the two SiNWs. So, we only show the rate-equation fit lines in Fig. 3(a) and (b), and the extracted lifetime using the exponential fits are shown in Fig. 3(c). The insets of Fig. 3(a) and (b) show the normalized dynamics for  $F = 50, 700 \mu\text{J}/\text{cm}^2$ , respectively. With increasing  $F$ , the decay for the bundled SiNWs (interconnected NWs in a single layer of SiNW sheet) clearly becomes slower, as shown in the inset of Fig. 3(a) and in the Fig. 3(c) extracted from the single exponential fit. From the simplest point of view, the  $-\Delta E/E_0$  dynamics arise from the decreased carrier density of the photoexcited carriers. When the surface-traps are saturated via high pump  $F$  excitation, the available trap density for the carriers to be captured is reduced; the relaxation kinetics follow a bulk-like indirect recombination, which results in slower relaxation with increasing  $F$  [18], [28]. This is the origin of the  $F$ -dependent relaxation for the bundled SiNWs.

For the individual SiNWs, see Fig. 3(b), while on the other hand, the decay shows nearly  $F$ -independent feature. The normalized dynamics in the inset of Fig. 3(b) seemingly shows that there are no variations of decay times with  $F$ . Because the transverse length is significantly smaller than the THz probe, it is expected that there must exist a new decay channel other than the surface trap-mediated recombination. One distinct point of the transverse dynamics for the individual NWs, apart from the longitudinal as well as from the bundled NWs dynamics, is that the excited carriers can be scattered off more easily from the NW surface [29]. While the high probability of carrier backscattering can be understood as the non-Drude conductivity spectrum [2], [30], [31], the electron and hole correlations within transverse region lead to multi-particle Auger scattering, by which the electron and hole are recombined nonradiatively. Consequently, the surface trap-mediated recombination is counterbalanced by this Auger scattering, revealing suppressed decay time constant  $\tau$  in the individual SiNWs.

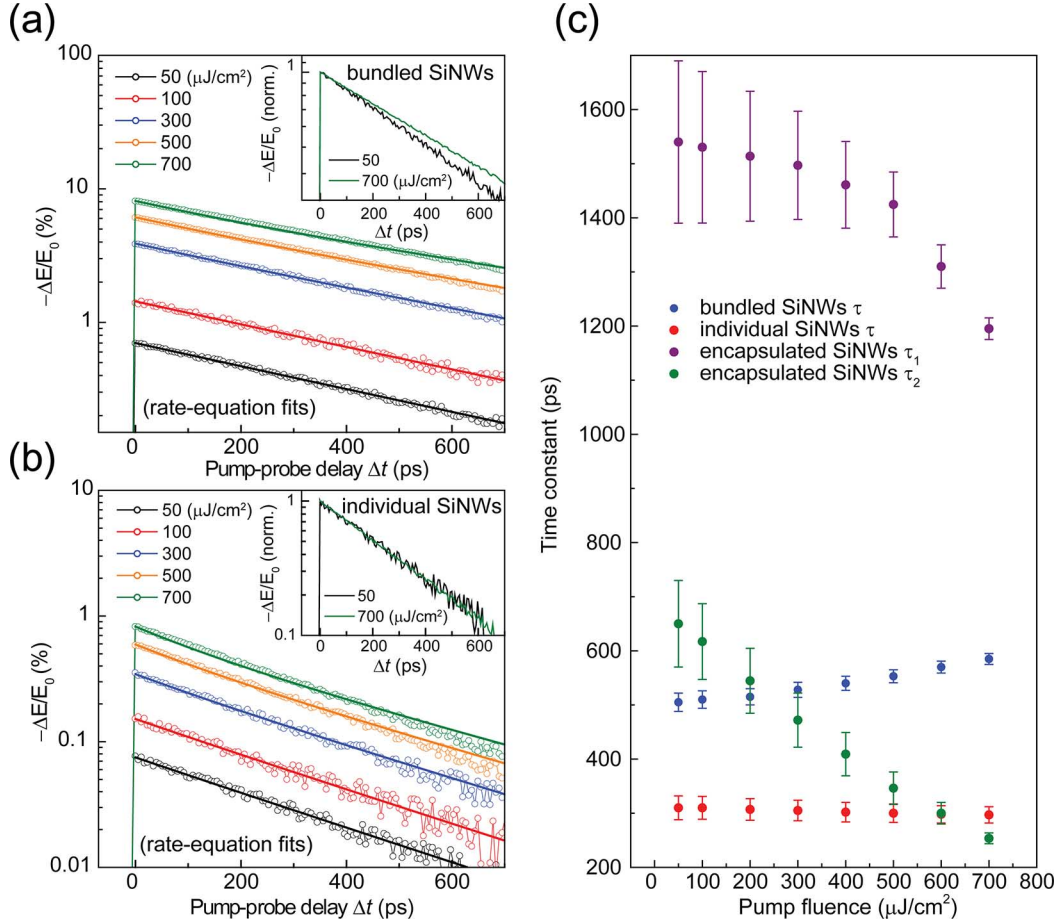


Fig. 3.  $F$ -dependent  $-\Delta E/E_0$  decay for the bundled (a) and for the individual SiNWs (b) are shown. Each inset in (a) and (b) is the normalized  $-\Delta E/E_0$  when  $F$  is 50 and 700  $\mu\text{J}/\text{cm}^2$ . The solid lines are the rate-equation fit as discussed in Section V. (c) Extracted time constants for the bundled SiNWs (blue circles), the individual bare (red circles), and the encapsulated SiNWs (purple circles for  $\tau_1$  and green circles for  $\tau_2$ ). The lifetimes are extracted from the single-exponential fit (bundled and individual SiNWs) and from the bi-exponential fit (encapsulated SiNWs).

Fig. 3(c) summarizes this characteristic  $F$ -dependent decay time constant  $\tau$  for the bundled, the individual, and the encapsulated SiNWs; for the encapsulated SiNWs, detailed discussions are provided in Section V. For the bundled SiNWs, the slow decay appears when  $F$  is larger than 100  $\mu\text{J}/\text{cm}^2$ . While the trap saturation leads to a slower relaxation for the bundled SiNWs, we emphasize that the same feature does not appear for the individual SiNWs. Rather,  $\tau$  is saturated at  $F > 100 \mu\text{J}/\text{cm}^2$ , suggesting that the Auger scattering in individual SiNWs reduces  $\tau$  with increasing  $F$ . This implies that the  $F$ -dependent Auger scattering counterbalances the slow carrier relaxation for the individual SiNWs, such that the effective  $\tau$  exhibits a nearly  $F$ -independent feature [32]. There might be a possibility of contributing a long-standing free-carrier lifetime of bulk Si ( $\sim 1 \mu\text{s}$ ) to the measured transient  $\Delta E/E$  response of the SiNWs. If the lifetime is long enough compared to the pulse-to-pulse 250 kHz repetition rate of our laser system, the photoinduced THz response would continuously add up, eventually no  $\Delta E/E$  response will be observed. Prior optical pump-probe measurements on the 160–210 nm SiNWs, however, have shown that the photoexcited free carriers experience rapid diffusion of electrons and holes, leading to a fast surface recombination with  $\sim 10^4 \text{ cm/s}$  velocity [13].

For more quantitative analysis, we have calculated the diffusion length from the measured decay constant. In our individual SiNWs, given the longest free-carrier lifetime of 300 ps and the diffusion constant of 24  $\text{cm}^2/\text{s}$ , we obtained the diffusion length of 0.85  $\mu\text{m}$  and the surface recombination velocity of  $0.4 \times 10^5 \text{ cm/s}$ , which is comparable to the previous investigations [11]. This suggests that the excited carriers are scattered off the surface at least once (on average) before they are recombined. For the possible contribution from the long lifetime of trap states, Gabriel *et al.* explicitly measured the trap state lifetime using the near-field pump-probe microscopy [13], and showed that the lifetime is about a few ns. So, we can conclude that neither the bulk-like long relaxation time nor the nanosecond trap lifetime does not add onto our  $\Delta E/E$  responses. For the bundled SiNWs, due to the high NW-to-NW interconnection, the Auger recombination plays a minor role, and the excited carriers diffuse toward adjacent NWs which prevents the carrier-carrier scattering event.

As to be discussed in Section V, the decay dynamics for the encapsulated SiNWs, shown in Fig. 3(c), display a faster relaxation component with increasing  $F$ , as evident from the bi-exponential fit; a single-exponential fit does not reproduce the fast relaxation component.

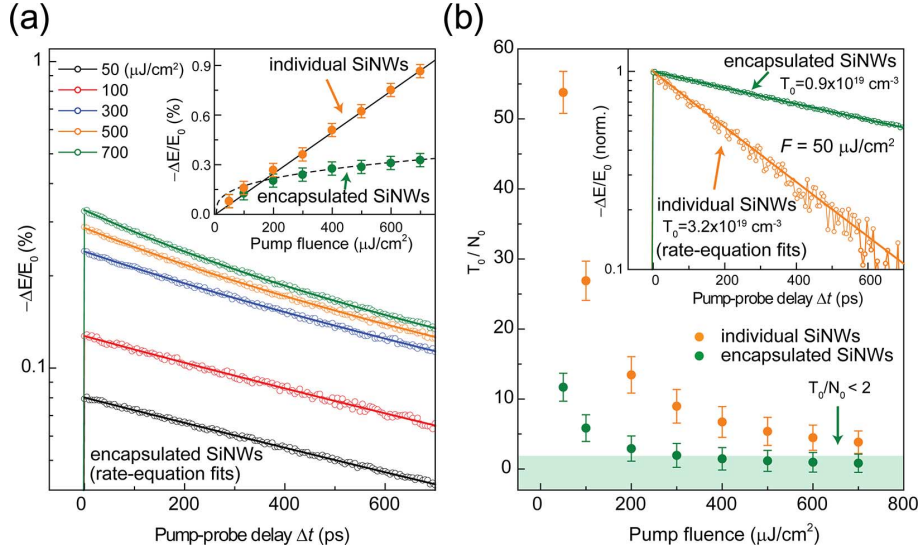


Fig. 4. (a) Transient  $-\Delta E/E_0$  decay for the encapsulated SiNWs with solid lines obtained from the rate-equation fits. Inset shows  $-\Delta E/E_0$  peak of encapsulated SiNWs as a function of  $F$ . Dashed fit line is obtained from numerical function proportional to  $F^{1/3}$ . For the individual SiNWs, it increases linearly as indicated by solid line. (b)  $F$ -dependent ratio between the initial unoccupied trap states  $T_0$  and the initial photoexcited carrier density  $N_0$  is shown for the bare individual SiNWs and for the encapsulated SiNWs. Inset: Normalized  $-\Delta E/E_0$  decay for the individual SiNWs and for the encapsulated SiNWs are shown when  $F$  is  $50 \mu\text{J}/\text{cm}^2$ . Solid lines are from the rate-equation fits.

## V. ENHANCED AUGER RECOMBINATION RATE IN ENCAPSULATED SiNWs

To clarify the effect of Auger scattering, we have reduced the surface-defect density by encapsulating the bare SiNWs by  $\text{SiO}_2$ . Since the majority of NW traps exist at the surface of NW [14], we expect that the trap-mediated decay is significantly suppressed when the NW surface is encapsulated. Fig. 4(a) shows the decay dynamics of the surface-encapsulated SiNWs with increasing the pump  $F$ . The carrier lifetime at  $F = 50 \mu\text{J}/\text{cm}^2$  of the encapsulated SiNWs is around 1.1 ns, which is indeed much longer than that of the individual SiNWs. Reduction of the trap density leads the diffusion length  $L$  to be increased to approximately  $1.6 \mu\text{m}$ . Intuitively, it means that carriers are scattered off the NW surface at least three times before recombination in a 500 nm diameter SiNW.

While the dynamics at  $F = 50 \mu\text{J}/\text{cm}^2$  represents a simple exponential decay, a noticeable transformation is the sharp increase of the decay rate at  $F = 700 \mu\text{J}/\text{cm}^2$ . The Auger recombination is evidenced via the fast initial decay with increasing  $F$ . While the initial relaxation at  $\Delta t < 150$  ps is faster than that of the trap-mediated recombination in the bundled SiNWs, a much slower decay component is observed at  $\Delta t > 150$  ps. Inset of Fig. 4(a), which is the peaks of  $-\Delta E/E_0$  with increasing  $F$ , shows that the  $-\Delta E/E_0$  peak is proportional to the third order of  $F$  for the encapsulated SiNWs, but it increases linearly for the individual SiNWs. Since we used the pump pulse energy of 1.55 eV which is higher than Si indirect bandgap ( $\sim 1.1$  eV), the excess energy of conduction band carriers in SiNWs are thermalized through electron-electron scattering (thermalization time of 120 fs) or electron-phonon scattering (thermalization time of 1 ps) [33]. The initial fast carrier-carrier scattering process beyond THz probe time resolution ( $\sim 1$  ps) leads to nonradiative carrier recombination, suppressing the  $-\Delta E/E_0$  increase at high  $F$ . For the encapsulated SiNWs, because the available

trap density is significantly reduced, the rapidly increased decay rates at early  $\Delta t$  imply that a new carrier recombination channel is opened. From the observed third-order  $F$  dependence, we attribute the new relaxation channel to the multi-particle Auger-type scattering. This  $F$ -dependent behavior is indeed quite different from the individual SiNWs, where the linear increasing  $F$ -dependent behavior in individual SiNWs primarily is due to the trap-mediated recombination. Here, we note that it does not mean that no Auger scattering is present in the individual SiNWs. As discussed in the below rate-equation analysis, the effect of Auger is relatively weak in the individual SiNWs, such that the trap-mediated recombination is dominant in the individual SiNWs. These analyses confirm that the Auger recombination is dominant in the surface encapsulated SiNWs at early pump-probe delay.

Now, an important issue is to compare the effect of Auger recombination between the individual and the encapsulated SiNWs, where the initial surface trap density is different. For quantitative comparison, we have constructed a rate-equation model that accounts for trap-mediated carrier recombination and Auger recombination. Our model is essentially a coupled rate-equation which consists of the density of excited charge carriers  $N$  and the density of unoccupied trap states  $T$  [18]

$$\frac{dN}{dt} = -\frac{N}{\tau_{\text{bulk}}} - \beta NT - C_2 N^2 \quad (3)$$

$$\frac{dT}{dt} = -\beta NT, \quad (4)$$

$$N(0) = N_0 \quad (5)$$

$$T(0) = T_0 \quad (6)$$

Here,  $N(0) = N_0$  is the initially photogenerated carrier density.

We estimate  $N_0 = F\sigma_{1.55 \text{ eV}}/N$ , where  $\sigma_{1.55 \text{ eV}}$  is the absorption cross-section of SiNW at 1.55 eV pump-photon energy and

TABLE I  
FITTING PARAMETERS USED FOR THE RATE-EQUATION FITS

	$\tau_{\text{bulk}}$	$\beta$ (cm <sup>3</sup> /s)	$C_2$ (cm <sup>3</sup> /s)	$T_0$ (cm <sup>-3</sup> )
bundled SiNWs	1 $\mu$ s	$1.0 \times 10^{-10}$	0	$2.0 \times 10^{19}$
individual SiNWs	1 $\mu$ s	$1.0 \times 10^{-10}$	$1.0 \times 10^{-10}$	$3.2 \times 10^{19}$
encapsulated SiNWs	1 $\mu$ s	$1.0 \times 10^{-10}$	$1.0 \times 10^{-10}$	$0.9 \times 10^{19}$

$V$  is the volume of the SiNW. Since no quantum confinement effect is expected in our SiNWs (the exciton Bohr radius is around 5 nm [34], [35], we have used a linear absorption cross-section model which assumes the photoexcitation takes place far from the band edge. In the expression, absorption cross-section  $\sigma_{1.55 \text{ eV}} = 1.43 \times 10^{-8} \text{ cm}^2$  is given by the (1). Here the values of  $N_0$  for the individual and encapsulated SiNWs are the same with  $0.77 \times 10^{18} \text{ cm}^{-3}$ ,  $1.54 \times 10^{18} \text{ cm}^{-3}$ ,  $4.62 \times 10^{18} \text{ cm}^{-3}$ ,  $7.7 \times 10^{18} \text{ cm}^{-3}$ , and  $10.8 \times 10^{18} \text{ cm}^{-3}$  at the pump fluence 50, 100, 300, 500 and 700  $\mu\text{J}/\text{cm}^2$ , respectively; these values are the same because the areal NW density for the two SiNWs is same with 3%. The trap density  $T(0)$  for the bundled SiNWs is  $T_0 = 2 \times 10^{19} \text{ cm}^{-3}$  and for the individual SiNWs is  $T_0 = 3.2 \times 10^{19} \text{ cm}^{-3}$ , whose values are obtained from the rate-equation fit. The difference between the two  $T_0$  can be explained by the fact that the bundled SiNWs are more connected with each other, exhibiting small density of trap states. The first term in the (3) describes the bulk indirect recombination with a time constant  $\tau_{\text{bulk}} \cong 1 \mu\text{s}$ , which was extracted from the  $-\Delta E/E_0$  decay of the bulk Si [Fig. 2(c)]. The second term in the (3) is related to saturable trap mediated recombination. This term depicts the carrier trapping to the available surface-traps with a coupling constant  $\beta$ . Such carrier trap reduces the free trap density  $T$  by an equal amount (as indicated in the (4)) with the initial trap density  $T_0$  being the total density of traps. The last term in (3) represents the Auger-type scattering process, and this term is incorporated to fit only the individual and the encapsulated SiNWs because no Auger-type recombination involves in the bundled SiNWs. The fitting parameters for the rate-equation model are summarized in the Table I.

Given the same  $F$ -excitation, the effect of trap density  $T_0$  on the individual and encapsulated SiNWs can be visualized if we plot the relative ratio between the trap density  $T_0$  and the photoexcited carrier density  $N_0$ . For this quantitative analysis, the above rate-equation model was used to fit the all the  $-\Delta E/E_0$  dynamics for the bundled (Fig. 3(a) without  $C_2$ ), individual (Fig. 3(b) with  $C_2$ ), and encapsulated SiNWs (Fig. 4(a) with  $C_2$ ). From the fitting results, we extracted the ratio  $T_0/N_0$  between the trap density  $T_0$  and the photoexcited carrier density  $N_0$ , as a function of  $F$  which is shown in Fig. 4(b). Here in the rate-equation analysis, we assumed that both the Auger recombination  $C_2$  and trap-mediated coupling  $\beta$  are presented in the individual and encapsulated SiNWs. For the individual SiNWs, the ratio  $T_0/N_0$  is large for the low  $F$ , due to the large amount of  $T_0$  and that for the encapsulated SiNWs is very small. With increasing  $F$ , the  $T_0/N_0$  ratio is decreased and the Auger recombination overwhelms the trap-mediated relaxation for the encapsulated SiNWs. We note that although similar trend is observed for the individual SiNWs, it does not mean that the Auger

effect is dominant. For example, when the ratio is below 2 (see the gray area), i.e., the photoexcited carrier density is even half of the trap density, one can see that the trap density is easily saturated for the encapsulated SiNWs, so that the Auger recombination is dominant. This effect is clearly pronounced for the encapsulated SiNWs than for the individual SiNWs. Although the Auger-induced initial fast decay is not clearly seen in the time-resolved data (see, for example  $F = 50 \mu\text{J}/\text{cm}^2$  in the Fig. 4(a) and in the inset of Fig. 4(b)), we note that this is not because the Auger scattering is ineffective, but because the Auger dynamics does not fully counterbalance the surface-trapping dynamics. Inset of Fig. 4(b) shows that the extracted  $T_0$  for the encapsulated SiNWs is approximately one fourth smaller than that of the individual SiNWs. As expected, because the trap density is significantly reduced for the encapsulated SiNWs, the decay dynamics is much slower than that of the individual SiNWs. As discussed in Fig. 3(c), there we corroborated that the Auger-type recombination was seen only from the encapsulated SiNWs, in which a successful fit can be obtained only when we use the bi-exponential function. The fast relaxation component of bi-exponential fit indicates that the Auger scattering is evident with decreasing the trap density.

## VI. CONCLUSION

In conclusion, we have investigated the carrier recombination dynamics of SiNWs along the transverse direction. For the systematic investigation, we have measured the THz carrier dynamics for the bundled SiNWs, individual bare SiNWs, and surface-encapsulated SiNWs. With increasing  $F$ , the decay dynamics for the bundled NWs becomes slower due to the pump-induced trap saturation. The individual SiNWs exhibits  $F$ -independent decay rate because the Auger recombination effectively reduces the saturation of trap states. When the defect density is reduced, we have clearly observed the Auger dynamics from the encapsulated SiNWs which arise due to increased carrier-carrier scattering event. For quantitative interpretation, we presented the two-level rate equation model to compare trap density and photoexcited carriers. Our studies on the ultrafast carrier relaxation pathways have made important contributions to the development of novel NW-based optoelectronic devices.

## REFERENCES

- [1] B. Tian, X. Zheng, T. J. Kempa, Y. Fang, N. Yu, G. Yu, J. Huang, and C. M. Lieber, "Coaxial silicon nanowires as solar cells and nanoelectronic power sources," *Nature*, vol. 449, no. 7164, pp. 885–889, Oct. 2007.
- [2] M. Lim, S.-J. Choi, G.-S. Lee, M.-L. Seol, Y. Do, Y.-K. Choi, and H. Han, "Terahertz time-domain spectroscopy of anisotropic complex conductivity tensors in silicon nanowire films," *Appl. Phys. Lett.*, vol. 100, no. 21, p. 211102, 2012.
- [3] R. P. Prasankumar, S. Choi, S. A. Trugman, S. T. Picraux, and A. J. Taylor, "Ultrafast electron and hole dynamics in germanium nanowires," *Nano Lett.*, vol. 8, no. 6, pp. 1619–1624, June 2008.
- [4] H. Fang, X. Li, S. Song, Y. Xu, and J. Zhu, "Fabrication of slantingly-aligned silicon nanowire arrays for solar cell applications," *Nanotechnology*, vol. 19, no. 25, p. 255703, Jun. 2008.
- [5] Y.-G. Jeong, M. J. Paul, S.-H. Kim, K.-J. Yee, D.-S. Kim, and Y.-S. Lee, "Large enhancement of nonlinear terahertz absorption in intrinsic GaAs by plasmonic nano antennas," *Appl. Phys. Lett.*, vol. 103, no. 17, p. 171109, 2013.
- [6] A. Pashkin, F. Junginger, B. Mayer, C. Schmidt, O. Schubert, D. Brida, R. Huber, and A. Leitenstorfer, "Quantum physics with ultrabroadband and intense terahertz pulses," *IEEE J. Sel. Topics Quantum Electron.*, vol. 19, no. 1, Jan. 2013, Art# 8401608.

- [7] I. Chatzakis, P. Tassin, L. Luo, N. Shen, L. Zhang, J. Wang, T. Koschny, and C. M. Soukoulis, "One- and two-dimensional photo-imprinted diffraction gratings for manipulating terahertz waves," *Appl. Phys. Lett.*, vol. 103, no. 4, 2013, Art# 043101.
- [8] K. Peng, X. Wang, and S.-T. Lee, "Silicon nanowire array photoelectrochemical solar cells," *Appl. Phys. Lett.*, vol. 92, no. 16, 2008, Art# 163103.
- [9] L. Tsakalakos, J. Balch, J. Fronheiser, B. A. Korevaar, O. Sulima, and J. Rand, "Silicon nanowire solar cells," *Appl. Phys. Lett.*, vol. 91, no. 23, 2007, Art# 233117.
- [10] J. H. Strait, P. A. George, M. Levendorf, M. Blood-forsythe, F. Rana, and J. Park, "Measurements of the carrier dynamics and terahertz response of oriented germanium nanowires using optical-pump terahertz probe spectroscopy," *Nano Lett.*, vol. 9, no. 8, pp. 2967–2972, 2009.
- [11] M. A. Seo, S. A. Dayeh, P. C. Upadhyaya, J. A. Martinez, B. S. Swartzentruber, S. T. Picraux, A. J. Taylor, and R. P. Prasankumar, "Understanding ultrafast carrier dynamics in single quasi-one-dimensional Si nanowires," *Appl. Phys. Lett.*, vol. 100, no. 7, 2012, Art# 071104.
- [12] H. Tang, L.-G. Zhu, L. Zhao, X. Zhang, J. Shan, and S.-T. Lee, "Carrier dynamics in Si nanowires fabricated by metal-assisted chemical etching," *ACS Nano*, vol. 6, no. 9, pp. 7814–7819, 2012.
- [13] M. M. Gabriel, J. R. Kirschbrown, J. D. Christesen, C. W. Pinion, D. F. Ziegler, E. M. Grumstrup, B. P. Mehl, E. E. M. Cating, J. F. Cahoon, and J. M. Papanikolas, "Direct imaging of free carrier and trap carrier motion in silicon nanowires by spatially-separated femtosecond pump-probe microscopy," *Nano Lett.*, vol. 13, no. 3, pp. 1336–1340, 2013.
- [14] R. Ulbricht, R. Kurstjens, and M. Bonn, "Assessing charge carrier trapping in silicon nanowires using picosecond conductivity measurements," *Nano Lett.*, vol. 12, no. 7, pp. 3821–3827, July 2012.
- [15] M. A. Seo, J. Yoo, S. A. Dayeh, S. T. Picraux, A. J. Taylor, and R. P. Prasankumar, "Mapping carrier diffusion in single silicon core-shell nanowires with ultrafast optical microscopy," *Nano Lett.*, vol. 12, no. 12, pp. 6334–6338, Dec. 2012.
- [16] M. R. Bergren, C. E. Kendrick, N. R. Neale, J. M. Redwing, R. T. Collins, T. E. Furtak, and M. C. Beard, "Ultrafast electrical measurements of isolated silicon nanowires and nanocrystals," *J. Phys. Chem. Lett.*, vol. 5, no. 12, pp. 2050–2057, 2014.
- [17] D. A. Wheeler, J.-A. Huang, R. J. Newhouse, W.-F. Zhang, S.-T. Lee, and J. Z. Zhang, "Ultrafast exciton dynamics in silicon nanowires," *J. Phys. Chem. Lett.*, vol. 3, no. 6, pp. 766–771, Mar. 2012.
- [18] P. Parkinson, H. J. Joyce, Q. Gao, H. H. Tan, X. Zhang, J. Zou, C. Jagadish, L. M. Herz, and M. B. Johnston, "Carrier lifetime and mobility enhancement in nearly defect-free core-shell nanowires measured using time-resolved terahertz spectroscopy," *Nano Lett.*, vol. 9, no. 9, pp. 3349–3353, 2009.
- [19] Y. J. Zhang, W. Li, and K. J. Chen, "Application of two-dimensional polystyrene arrays in the fabrication of ordered silicon pillars," *J. Alloys Compd.*, vol. 450, no. 1, pp. 512–516, Feb. 2008.
- [20] Z. Huang, H. Fang, and J. Zhu, "Fabrication of silicon nanowire arrays with controlled diameter, length, and density," *Adv. Mater.*, vol. 19, no. 5, pp. 744–748, Mar. 2007.
- [21] J. Seo, S. Lee, H. Han, Y. Chung, J. Lee, S.-D. Kim, Y.-W. Kim, S. Lim, and T. Lee, "Reversible wettability control of silicon nanowire surfaces: From superhydrophilicity to superhydrophobicity," *Thin Solid Films*, vol. 527, pp. 179–185, Jan. 2013.
- [22] S. Lee, J. H. Koo, J. Seo, S.-D. Kim, K. H. Lee, S. Im, Y.-W. Kim, and T. Lee, "The effects of surface modification on the electrical properties of p-n+ junction silicon nanowires grown by an aqueous electroless etching method," *J. Nanoparticle Res.*, vol. 14, no. 840, Apr. 2012.
- [23] J. Giblin, V. Protasenko, and M. Kuno, "Wavelength sensitivity of single nanowire excitation polarization anisotropies explained through a generalized treatment of their linear absorption," *ACS Nano*, vol. 3, no. 7, pp. 1979–1987, Jul. 2009.
- [24] D. E. Aspnes and A. A. Studna, "Dielectric functions and optical parameters of Si, Ge, GaP, GaAs, GaSb, InP, InAs, and InSb from 1.5 to 6.0 eV," *Phys. Rev. B*, vol. 27, no. 2, pp. 985–1009, 1983.
- [25] I. Robel, B. A. Bunker, P. V. Kamat, and M. Kuno, "Exciton recombination dynamics in CdSe nanowires: Bimolecular to three-carrier Auger kinetics," *Nano Lett.*, vol. 6, no. 7, pp. 1344–1349, July 2006.
- [26] V. V. Protasenko, K. L. Hull, and M. Kuno, "Disorder-induced optical heterogeneity in single CdSe nanowires," *Adv. Mater.*, vol. 17, no. 24, pp. 2942–2949, Dec. 2005.
- [27] A. Kar, P. C. Upadhyaya, S. A. Dayeh, S. T. Picraux, S. Member, A. J. Taylor, and R. P. Prasankumar, "Probing ultrafast carrier dynamics in silicon nanowires," *IEEE J. Sel. Topics Quantum Electron.*, vol. 17, no. 4, pp. 889–895, 2011.
- [28] P. Uhd Jepsen, W. Schairer, I. H. Libon, U. Lemmer, N. E. Hecker, M. Birkholz, K. Lips, and M. Schall, "Ultrafast carrier trapping in microcrystalline silicon observed in optical pump-terahertz probe measurements," *Appl. Phys. Lett.*, vol. 79, no. 9, pp. 1291–1293, 2001.
- [29] J. Kim, I. Maeng, J. Jung, H. Song, J.-H. Son, K. Kim, J. Lee, C.-H. Kim, G. Chae, M. Jun, Y. Hwang, S. Jeong Lee, J.-M. Myoung, and H. Choi, "Terahertz time-domain measurement of non-Drude conductivity in silver nanowire thin films for transparent electrode applications," *Appl. Phys. Lett.*, vol. 102, no. 1, 2013, Art 011109.
- [30] Y. Tsai, C. Chang, Y. Lai, P. Yu, and H. Ahn, "Realization of metal-insulator transition and oxidation in silver nanowire percolating networks by terahertz reflection spectroscopy," *ACS Appl. Mater. Interfaces*, vol. 6, no. 1, pp. 630–635, 2013.
- [31] D. Cooke, A. MacDonald, A. Hryciw, J. Wang, Q. Li, A. Meldrum, and F. Hegmann, "Transient terahertz conductivity in photoexcited silicon nanocrystal films," *Phys. Rev. B*, vol. 73, no. 19, p. 193311, May 2006.
- [32] A. Esser, K. Seibert, H. Kurz, G. N. Parsons, C. Wang, B. N. Davidson, G. Lucovsky, and R. J. Nemanich, "Ultrafast recombination and trapping in amorphous silicon," *Phys. Rev. B*, vol. 41, no. 5, pp. 2879–2884, 1990.
- [33] J. R. Godman and J. A. Prybyla, "Ultrafast dynamics of laser-excited electron distributions in silicon," *Phys. Rev. Lett.*, vol. 72, no. 9, pp. 1364–1367, 1994.
- [34] D. L. Smith, D. S. Pan, and T. C. McGill, "Impact ionization of excitons in Ge and Si," *Phys. Rev. B*, vol. 12, no. 10, pp. 4360–4366, 1975.
- [35] D. D. D. Ma, C. S. Lee, F. C. K. Au, S. Y. Tong, and S. T. Lee, "Small-diameter silicon nanowire surfaces," *Science*, vol. 299, no. 5614, pp. 1874–1877, Mar. 2003.



**Chihun In** received the B.S. degree in electrical and electronic engineering from Yonsei University, Seoul, Korea, in 2014.

He is currently with the School of Electrical and Electronic Engineering, Yonsei University, Seoul, Korea, as a graduate student researcher.



**Jungmok Seo** received the B.S. and Ph.D. degrees in electrical and electronic engineering from Yonsei University, Seoul, Korea, in 2008 and 2014, respectively.

He is currently with the School of Electrical and Electronic Engineering, Yonsei University, Seoul, Korea, as a postdoctoral research fellow.



**Hyukho Kwon** received the B.S. and M.S. degrees in electrical and electronic engineering from Yonsei University, Seoul, Korea, in 2012 and 2014, respectively.

He is currently with Samsung Electronics Company, Banwoldong, Hwaseongsi, Gyeonggido, Korea as an Assistant Engineer.



**Jeongmook Choi** received the B.S. and M.S. degrees in electrical and electronic engineering from Yonsei University, Seoul, Korea, in 2014 and 2014, respectively.

He is currently with LG Display Company, Wol-longmyeon, Pajusi, Gyeonggido, Korea, as an Assistant Engineer.



**Sangwan Sim** received the B.S. degree in electrical and electronic engineering from Yonsei University, Seoul, Korea in 2013, and is currently working toward the Ph.D. degree in electrical and electronic engineering from Yonsei University, Seoul, Korea.



**Jaeseok Kim** received the B.S. and the M.S. degrees in electrical and electronic both from Yonsei University, Seoul, Korea, in 2011 and 2013, respectively, and is currently working toward the Ph.D. degree in electrical and electronic engineering.



**Taeyong Kim** received the B.S. degree in electrical and electronic engineering in Yonsei University, Seoul, Korea in 2013.

He is currently with the Department of Electrical Engineering, California Institute of Technology, Pasadena, CA, USA, as a graduate student researcher.



**Taeyoon Lee** received the B.S. and M.S. degrees in metallurgical system engineering from Yonsei University, Seoul, Korea, in 1995 and 1997, respectively, and the Ph.D. degree in materials science and engineering from the University of Illinois at Urbana Champaign, Champaign, IL USA, in 2004.

He joined Intel Corporation as a Senior Process Engineer in the Flash Memory Group in 2005, and worked there for 3 years, where he gained extensive research and development experience in nonvolatile memory device and integrated chip manufacturing.

He is currently an Associate Professor in the School of Electrical and Electronic Engineering, Yonsei University, Seoul, Korea. His research interests include exploring 1-D and 2-D nanobuilding blocks, novel devices including nanowires (Si, SiGe, ZnO, etc.) and carbon materials (carbon nanotube, graphene, and graphene oxide). Furthermore, he also has interest in bio-inspired smart surfaces, ultrathin blocking barrier, and flexible electronics.



**Hyunyoung Choi** received the B.S. degree in electrical and electronic engineering from Yonsei University, Seoul, Korea, in 2002, and the M.S. and Ph.D. degrees in electrical engineering and computer science from the University of Michigan, Ann Arbor, MI, USA, in 2004 and 2007, respectively.

After a postdoctoral position at Lawrence Berkeley National Laboratory, Berkeley, CA USA (2008–2010), he joined Yonsei University, Seoul, Korea, as an Assistant Professor in 2011. His research interests include ultrafast optical and tera-

hertz spectroscopy, and its application to the optoelectronic devices, such as nanowire, graphene, metamaterial, topological insulator, and 2-D materials.